JACS
JOURNAL OF THE AMERICAN CHEMICAL SOCIETY

ARTICLE

pubs.acs.org/JACS

Syntheses and Structural Characterizations of Anionic Borane-Capped Ammonia Borane Oligomers: Evidence for Ammonia Borane H_2 Release via a Base-Promoted Anionic Dehydropolymerization Mechanism

William C. Ewing, Allegra Marchione, Daniel W. Himmelberger, Patrick J. Carroll, and Larry G. Sneddon*

Department of Chemistry, University of Pennsylvania, Philadelphia, Pennsylvania 19104-6323, United States

Supporting Information

ABSTRACT: Studies of the activating effect of Verkade's base, 2,8,9-triisobutyl-2,5,8,9-tetraaza-1-phosphabicyclo[3.3.3]undecane (VB), on the rate and extent of H_2 release from ammonia borane (AB) have led to the syntheses and structural characterizations of three anionic aminoborane chain-growth products that provide direct support for anionic dehydropolymerization mechanistic steps in the initial stages of base-promoted AB H_2 release reactions. The salt $VBH^+[H_3BNH_2BH_2NH_2BH_3]^-$ (**1**) containing a linear five-membered anionic aminoborane chain was produced in 74% yield via the room-temperature reaction of a 3:1 AB/VB mixture in fluorobenzene solvent, while the branched and linear-chain seven-membered anionic aminoborane oligomers $VBH^+[HB(NH_2BH_3)_3]^-$ (**2a**) and $VBH^+[H_3BNH_2BH_2NH_2BH_2NH_2BH_3]^-$ (**2b**) were obtained from VB/AB reactions carried out at 50 °C for 5 days when the AB/VB ratio was increased to 4:1. X-ray crystal structure determinations confirmed that these compounds are the isoelectronic and isostructural analogues of the hydrocarbons *n*-pentane, 3-ethylpentane, and *n*-heptane, respectively. The structural determinations also revealed significant interionic B−H···H−N dihydrogen-bonding interactions in these anions that could enhance dehydrocoupling chain-growth reactions. Such mechanistic pathways for AB H_2 release, involving the initial formation of the previously known $[H_3BNH_2BH_3]^-$ anion followed by sequential dehydrocoupling of B−H and H−N groups of growing borane-capped aminoborane anions with AB, are supported by the fact that **1** was observed to react with an additional AB equivalent to form **2a** and **2b**.

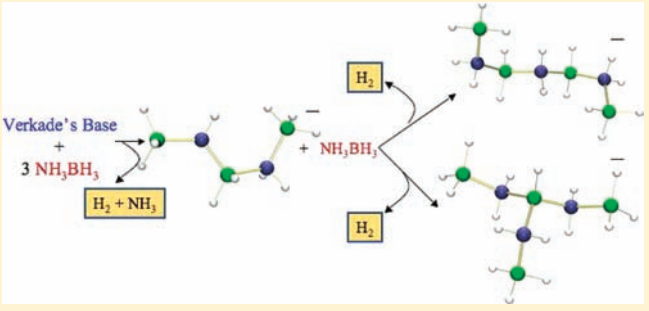

INTRODUCTION

Because of its high hydrogen content (19.6 wt %) and recently demonstrated regenerability,[1] ammonia borane (H_3NBH_3, AB) continues to be one of the most promising materials for a chemical hydride-based hydrogen storage system for transportation applications.[2] Recent studies have focused on increasing the rate and extent of H_2 delivery from AB and have demonstrated that AB H_2 release can be initiated using a variety of strategies, including activation by nano- and mesoporous scaffolds,[3] acids,[4] bases,[5] ionic liquids,[6] or transition-metal catalysts,[7] and a number of distinctly different mechanistic pathways for activated AB H_2 release have now been proposed.

We previously reported[5] that bases such as bis(dimethylamino)naphthalene [proton sponge (PS)] can be used to promote H_2 release from AB. On the basis of the spectroscopic data for the PS/AB reactions and model studies of the reactions of the $[Et_3BNH_2BH_3]^-$ anion with AB, the base-promoted AB H_2 release reactions were proposed to proceed initially via an anionic dehydropolymerization mechanism to produce growing anionic polyaminoborane polymers. We report in this paper the syntheses and structural characterizations of borane-capped anionic polyaminoborane oligomeric products from the reactions of AB with Verkade's base, 2,8,9-triisobutyl-2,5,8,9-tetraaza-1-phosphabicyclo[3.3.3]undecane[8] ($C_{18}H_{39}N_4P$, VB), that provide additional strong evidence in support of such anionic chain-growth pathways in the initial stages of base-promoted AB H_2 release.

EXPERIMENTAL SECTION

All preparations were carried out using standard high-vacuum or inert-atmosphere techniques, as described by Shriver.[9]

Materials. AB (Aviabor, 97% minimum purity) was ground into a free-flowing powder using a commercial coffee grinder. VB (Sigma-Aldrich, ~97%) was dried under high vacuum and stored in a nitrogen-filled glovebox. The ionic liquid 1-butyl-3-methylimidazolium chloride (bmimCl) (Fluka) was dried by toluene azeotropic distillation. Fluorobenzene (Aldrich) was dried over CaH_2 and stored over Linde 4 Å molecular sieves. Toluene and diethyl ether (Fisher) were HPLC-grade and used as received.

Physical Measurements. Solution ^{11}B (Bruker UNI-400), ^1H (Bruker BioDRX-500 or Bruker UNI-400), and ^{31}P (Bruker DMX-300)

Received: August 23, 2011
Published: September 30, 2011

NMR spectra were collected at 25 °C. The ^{11}B chemical shifts were referenced to $BF_3 \cdot OEt_2$ (0.0 ppm), with a negative sign indicating an upfield shift. The proton chemical shifts were measured relative to internal residual protons from the lock solvents (99.9% CD_2Cl_2) and then referenced to $(CH_3)_4Si$ (0.0 ppm). The ^{31}P chemical shifts were referenced to 75% phosphoric acid, with a negative sign indicating an upfield shift. IR data were obtained on a PerkinElmer Spectrum 100 FT-IR spectrometer and are provided in Table S1 in the Supporting Information (SI). Elemental analyses were obtained at the MicroAnalytical Facility at UC Berkeley, CA.

Computational Studies. DFT/GIAO/NMR calculations were performed using the Gaussian 03 program.[10] Geometry optimizations were carried out at the B3LYP/6-311G(d) level (Figures S1−S6 and Table S3 in the SI), and the ^{11}B NMR chemical shifts were also calculated at the B3LYP/6-311G(d) level using the GIAO option in Gaussian 03 and referenced to $BF_3 \cdot OEt_2$ using an absolute shielding constant of 102.24 (Table S2 in the SI).

Procedures for Comparison H_2 Release Measurements. The Toepler pump system and procedures used for hydrogen measurements were identical to those described previously.[5,6] AB (250 mg, 8.1 mmol), bmimCl (250 mg), and either PS or VB (5 mol %) were loaded into 100 mL reaction flasks under N_2. The flasks were then evacuated, sealed, and placed in a hot oil bath preheated to 85 °C. The flasks were opened at the indicated times, and any gaseous products were passed through a liquid nitrogen trap before continuing on to the Toepler pump (700 mL), where the released H_2 was pumped into a series of calibrated volumes with the final pressure measured (±0.5 mm) with the aid of a U-tube manometer. Post reaction, the reaction flasks were evacuated for 30 min through the cold trap to remove any volatile products from the reaction residue. The product residues and volatiles in the cold trap were extracted with dry glyme and/or pyridine and analyzed by ^{11}B NMR spectroscopy.

Synthesis and Isolation of $[C_{18}H_{39}N_4PH^+][H_3BNH_2BH_2NH_2BH_3]^-$ (1). A stirring suspension of AB (0.10 g, 3.2 mmol) in fluorobenzene (10 mL) was reacted with VB (0.38 mL, 1.1 mmol) at room temperature until all of the solid AB had been dissolved and consumed (~3 days). With the solution cooled at 0 °C, the addition of heptane (15 mL) caused the precipitation of a white solid that was then collected via filtration. The solid was dissolved in warm toluene and recrystallized at −30 °C to yield pure **1** (330 mg, 0.80 mmol, 74%).

Data for **1**: Anal. Calcd: C, 51.92%; H, 12.50%; N, 20.19%. Found: C, 51.98%, H, 12.31%, N, 19.83%. ^{11}B NMR (128.3 MHz, $CDCl_3$): δ −8.8 (t, J = 101 Hz, BH_2), −22.3 (d, J = 91 Hz, $2BH_3$). ^{1}H{^{11}B} NMR (499.7 MHz, CD_2Cl_2): δ 5.20 (d, J_{P-H} = 503 Hz, 1P*H*), 3.28 (q, J = 5 Hz, $3CH_2$), 3.10 (m, $3CH_2$), 2.68 (dd, J = 8, 10 Hz, $3CH_2$), 2.07 (br s, $2NH_2$), 1.93 (br quin, J = 5 Hz, BH_2), 1.83 (sep, J = 8 Hz, 3C*H*), 1.28 (t, J = 4 Hz, $2BH_3$), 0.86 (d, J = 8 Hz, $6CH_3$). ^{31}P NMR (121.5 MHz, CD_2Cl_2): −6.6 (d, J_{P-H} = 499 Hz, *P*H).

Synthesis and Isolation of $[C_{18}H_{39}N_4PH^+][HB(NH_2BH_3)_3]^-$ (2a) and $[C_{18}H_{39}N_4PH^+][H_3BNH_2BH_2NH_2BH_2NH_2BH_3]^-$ (2b). A stirring suspension of AB (0.10 g, 3.2 mmol) in fluorobenzene (10 mL) was reacted with VB (0.28 mL, 0.8 mmol) at 50 °C for 5 days. The cloudy solution was diluted with CH_2Cl_2 (5 mL) and filtered. ^{11}B NMR analysis of the filtrate revealed the formation of **2a** and **2b** in a 2:1 ratio along with a small amount of **1**. The solvent was vacuum-evaporated, and the residual oil was washed with toluene, causing the precipitation of a white solid. The solid was washed twice with cold toluene and dried in vacuo to give **2a** (160 mg, 0.36 mmol, 32%). The supernatant solution was collected and the solvent then vacuum-evaporated, leaving a clear oil that solidified when washed with cold diethyl ether. This solid was redissolved in a small amount of a warm 1:1 mixture of toluene and diethyl ether and recrystallized at −20 °C, yielding **2b** (46 mg, 0.10 mmol, 9%).

Data for **2a**: Anal. Calcd.: C, 48.60%, H, 12.69%, N, 22.04%. Found: C, 48.4%, H, 12.89%, N, 21.69%. ^{11}B NMR (128.3 MHz, $CDCl_3$): δ −4.5 (d, J = 117 Hz, *B*H), −24.0 (d, J = 93 Hz, $2BH_3$). ^{1}H{^{11}B} NMR (400.1 MHz, CD_2Cl_2) (Figure S7 in the SI): δ 5.24 (d, J_{P-H} = 503 Hz, 1P*H*), 3.24 (q, J = 5 Hz, $3CH_2$), 3.12 (m, $3CH_2$), 2.72 (dd, J = 8, 10 Hz, $3CH_2$), 2.44 (br s, $3NH_2$), 2.20 (br s, J = 5 Hz, B*H*), 1.85 (sep, J = 8 Hz, 3C*H*), 1.22 (br s, $3BH_3$), 0.88 (d, J = 8 Hz, $6CH_3$). ^{31}P NMR (121.5 MHz, CD_2Cl_2): −6.3 (d, J_{P-H} = 487 Hz, *P*H).

Data for **2b**: ^{11}B NMR (128.3 MHz, $CDCl_3$): δ −10.7 (t, J = 100 Hz, $2BH_2$), −22.4 (d, J = 91 Hz, $2BH_3$). ^{1}H{^{11}B} NMR (400.1 MHz, CD_2Cl_2) (Figure S8 in the SI): δ 5.22 (d, J_{P-H} = 503 Hz, 1P*H*), 3.28 (q, J = 5 Hz, $3CH_2$), 3.11 (m, $3CH_2$), 2.70 (dd, J = 8, 10 Hz, $3CH_2$), 2.07 (br s, $2NH_2$), 1.96 (s, $2BH_2$), 1.85 (sep, J = 8 Hz, 3C*H*), 1.32 (br s, $2BH_3$), 0.87 (d, J = 8 Hz, $6CH_3$). ^{31}P NMR (121.5 MHz, CD_2Cl_2): −6.6 (d, J_{P-H} = 529 Hz, *P*H).

Reactions at 50 °C also always produced a small amount (<20 mg) of a CH_2Cl_2-insoluble white solid. This solid could be dissolved in *N*,*N*-dimethylformamide (DMF), and a ^{11}B NMR spectrum of this material is shown in Figure S9 in the SI.

Reaction of 1 with Ammonia Borane. **1** (190 mg, 0.46 mmol) was reacted with AB (15 mg, 0.50 mmol) in fluorobenzene (~10 mL) at 50 °C for 2 days. The solvent was vacuum-evaporated, and the resultant oil was then redissolved in CH_2Cl_2. Analysis by ^{11}B NMR spectroscopy (Figure S10 in the SI) indicated the formation of both **2a** and **2b** accompanied by the disappearance of **1**.

Crystallographic Data. Crystals of **1** were obtained by recrystallization in toluene. Crystals of **2a** and **2b** were obtained by recrystallization from mixtures of toluene and diethyl ether.

Collection and Reduction of the Data. Crystallographic data and structure refinement information are summarized in Table 1. The X-ray intensity data for **1** (UP3375), **2a** (UP3393), and **2b** (UP3374) were collected on a Bruker APEXII CCD area detector employing graphite-monochromatized Mo Kα radiation. Rotation frames were integrated using SAINT,[11] producing a list of unaveraged F^2 and $\sigma(F^2)$ values that were then passed to the SHELXTL[12] program package for further processing and structure solution on a Dell Pentium 4 computer. The intensity data were corrected for Lorentz and polarization effects and for absorption using SADABS.[13]

Solution and Refinement of the Structures. The structures were solved by direct methods (SIR97[14]). Refinement was by full-matrix least-squares based on F^2 using SHELXL-97.[15] All reflections were used during the refinement (values of F^2 that were experimentally negative were replaced with $F^2 = 0$). All non-hydrogen atoms were refined anisotropically, and hydrogen atoms were refined isotropically.

RESULTS AND DISCUSSION

In the course of screening the effectiveness of various strong bases for inducing ammonia borane H_2 release, we examined the reactions of AB with Verkade's base, 2,8,9-triisobutyl-2,5,8,9-tetraaza-1-phosphabicyclo[3.3.3]undecane.[8] VB is a sufficiently strong base[16] that it readily deprotonates AB to form the $H_3BNH_2^-$ anion, which is needed to initiate an AB anionic polymerization reaction. Although VB proved to be less effective in promoting AB H_2 release than proton sponge in ionic liquids, H_2 release measurements confirmed that the addition of 5 mol % VB to a 50:50 wt % AB/bmimCl mixture significantly increased both the rate and extent of AB H_2 release at 85 °C (Figure 1) relative to those reactions without any added base. ^{11}B NMR studies of VB/AB H_2 release reactions in progress showed product spectral patterns similar to those previously observed[5] in the PS/AB reactions, suggesting the formation of both linear and chain-branched anionic polyaminoborane polymers, as proposed for the PS/AB reactions.

In an attempt to isolate oligomeric aminoborane products from the VB/AB reactions, a 3:1 ratio of AB to VB was reacted

Table 1. Crystallographic Data

	1	2a	2b
empirical formula	$C_{18}B_3H_{52}N_6P$	$C_{18}B_4H_{56}N_7P$	$C_{18}B_4H_{56}N_7P$
formula weight	416.06	444.91	444.91
crystal class	triclinic	monoclinic	triclinic
space group	$P\bar{1}$	$P2_1/c$	$P\bar{1}$
Z	2	4	4
a (Å)	9.052(2)	17.8873(8)	8.3185(15)
b (Å)	9.299(2)	10.4153(5)	10.2544(19)
c (Å)	17.014(4)	15.5540(7)	36.740(6)
α (deg)	102.904(10)		85.455(9)
β (deg)	90.446(11)	101.029(2)	87.606(8)
γ (deg)	108.183(9)		66.520(8)
V (Å^3)	1321.6(5)	2844.2(2)	2865.3(9)
D_{calc} (g/cm^3)	1.045	1.039	1.031
μ, cm^{-1}	1.19	1.15	1.14
$\lambda_{Mo\ K\alpha}$ (Å)	0.71073	0.71073	0.71073
crystal size (mm)	0.40 × 0.30 × 0.05	0.30 × 0.30 × 0.10	0.36 × 0.32 × 0.18
F(000)	464	992	992
2θ (deg)	4.74−50.72	4.54−50.22	3.34−50.14
T (K)	143(1)	143(1)	143(1)
hkl collected	$-10 \le h \le 10$	$-21 \le h \le 20$	$-9 \le h \le 9$
	$-11 \le k \le 11$	$-12 \le k \le 12$	$-12 \le k \le 12$
	$-20 \le l \le 20$	$-18 \le l \le 18$	$-43 \le l \le 43$
no. of measured reflns	33133	37499	79920
no. of unique reflns	4708 (R_{int} = 0.0254)	5031 (R_{int} = 0.0249)	44167 (R_{int} = 0.0296)
no. of parameters	462	496	683
R indices ($F > 2\sigma$)[a]	R_1 = 0.0314, wR_2 = 0.0790	R_1 = 0.0315, wR_2 = 0.0791	R_1 = 0.0485, wR_2 = 0.1223
R indices (all data)[a]	R_1 = 0.0348, wR_2 = 0.0824	R_1 = 0.0367, wR_2 = 0.0829	R_1 = 0.0570, wR_2 = 0.1294
GOF[b]	0.923	0.990	0.980
final difference peaks (e/Å^3)	+0.268, −0.258	+0.257, −0.275	+1.232, −0.701

[a] $R_1 = \Sigma||F_o| - |F_c||/\Sigma|F_o|$; $wR_2 = [\Sigma w(F_o^2 - F_c^2)^2/\Sigma w(F_o^2)^2]^{1/2}$ [b] GOF = $[\Sigma w(F_o^2 - F_c^2)^2/(n-p)]^{1/2}$, where n is the number of reflections and p is the number of parameters refined.

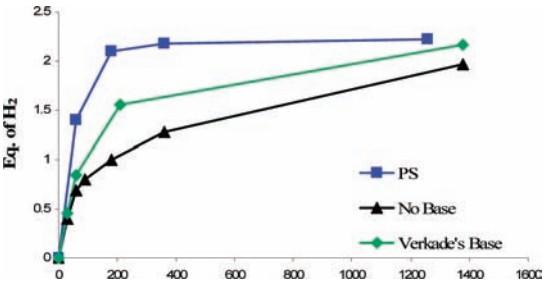

Figure 1. H_2 release at 85 °C from 50:50 AB/bmimCl mixtures without and with the addition of 5 mol % VB or PS.

in fluorobenzene at room temperature. Two new product resonances (an intensity-1 triplet at −8.8 ppm and an intensity-2 quartet at −22.3 ppm) emerged in the ^{11}B NMR spectrum of the reaction mixture, coinciding with the dissolution of the only slightly soluble AB. After ~3 days, all of the solid AB had dissolved and reacted. Addition of heptane to the reaction mixture induced the precipitation of a white solid that was then recrystallized from warm toluene to give VBH^+-$[H_3BNH_2BH_2NH_2BH_3]^-$ (**1**) in 74% yield (eq 1). An X-ray diffraction study of this salt (Figure 2) confirmed that it was composed of a linear five-membered anionic aminoborane chain and a VBH^+ cation.

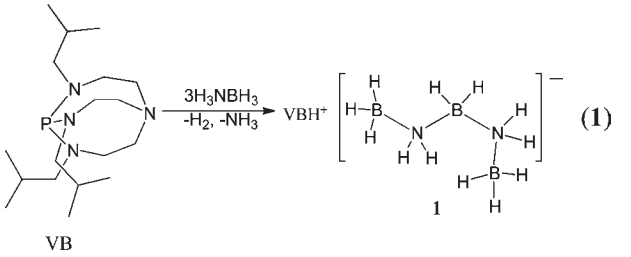

Additional product peaks were observed in the ^{11}B NMR spectra of VB/AB reactions carried out at 50 °C for 5 days when the ratio of AB to VB was increased to 4:1.[17] Two new anionic aminoborane/VBH^+ salts, along with a small amount of **1**, were isolated from this mixture by selective precipitation/crystallization. The crystallographic determinations of these products, $VBH^+[HB(NH_2BH_3)_3]^-$ (**2a**) (Figure 3) and VBH^+ $[H_3BNH_2BH_2NH_2BH_2NH_2BH_3]^-$ (**2b**) (Figure 4), confirmed the formation of both branched (**2a**) and linear chain (**2b**) seven-membered anionic aminoborane oligomers

dx.doi.org/10.1021/ja207971h |J. Am. Chem. Soc. 2011, 133, 17093–17099

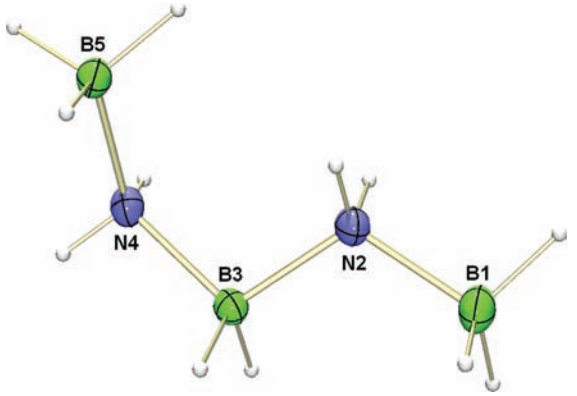

Figure 2. Crystallographically determined structure of the five-membered aminoborane anion in **1**. Selected bond distances (Å) and angles (deg): B1−N2, 1.591(2); N2−B3, 1.5631(18); B3−N4, 1.5762(18); N4−B5, 1.5984(18); B1−Ha,b,c, 1.13 (avg); B5−Ha,b,c, 1.13 (avg); B3−Ha,b, 1.12 (avg); N2−Ha,b, 0.86 (avg); N4−Ha,b, 0.87 (avg); B1−N2−B3, 117.58(11); N2−B3−N4, 108.47(10); B3−N4−B5 119.81(10).

as the result of the dehydrocoupling of one additional AB unit (eq 2).

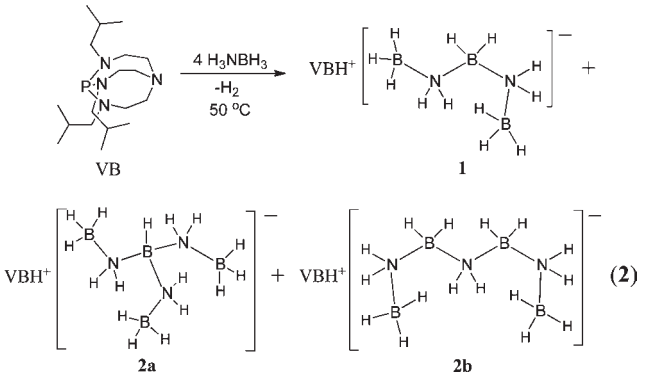

The anionic aminoboranes in **1**, **2a**, and **2b** are the respective isoelectronic and isostructural analogues of the hydrocarbons *n*-pentane, 3-ethylpentane, and *n*-heptane, and their bond angles (N−B−N, ∼107−109°, B−N−B, ∼117−119°) and distances at both boron and nitrogen are consistent with sp^3 hybridization. The average B−N bond lengths to the terminal boron atoms (**1**, 1.594 Å; **2a**, 1.599 Å; **2b**, 1.587 Å) in all three anions are significantly longer than the average lengths of B−N bonds to their internal borons (**1**, 1.569 Å; **2a**, 1.565 Å; **2b**, 1.574 Å), with these differences similar to those recently reported for the four-membered neutral $H_3BNH_2BH_2NH_3$ aminoborane chain analogue of butane (internal B−N, 1.567 Å; terminal B−N, 1.594 Å).[18] Also as in $H_3BNH_2BH_2NH_3$, the two linear anions (**1** and **2b**) take gauche configurations in the solid state, rather than the anti configuration seen for linear alkanes. This difference can be attributed to the stabilizing effect of intramolecular NH···HB dihydrogen-bonding interactions in the gauche structures of these anions (**1**, 2.196 Å avg; **2b**, 2.282 Å avg), and density functional theory (DFT) calculations at the B3LYP/6-311G(d) level for both of these anions confirmed the increased stability of their gauche conformations relative to the anti ones (**1**, gauche −3.48 kcal; **2a**, gauche −8.23 kcal; Table S3 and Figures S1−S6 in the SI).

As shown in Figure 5, the NMR spectra for **1**, **2a**, and **2b** are entirely consistent with their X-ray-determined structures. The

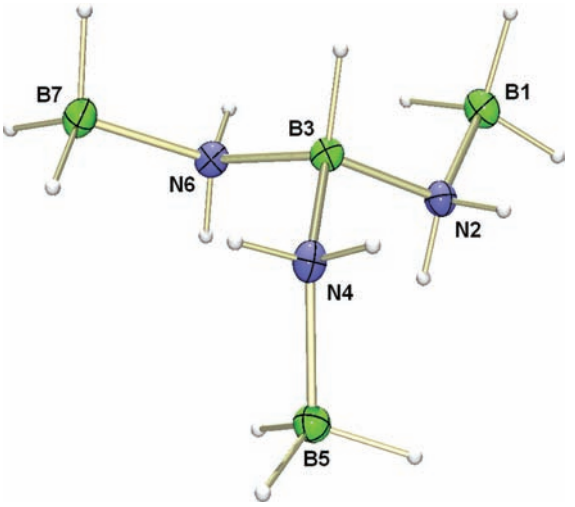

Figure 3. Crystallographically determined structure of the seven-membered branched-chain aminoborane anion in **2a**. Selected bond distances (Å) and angles (deg): B1−N2, 1.5965(17); N2−B3, 1.5622(17); B3−N4, 1.5724(16); N4−B5, 1.6113(17); B3−N6, 1.5610(16); N6−B7, 1.5904(17); B1−Ha,b,c, 1.14 (avg); B7−Ha,b,c, 1.23 (avg); B3−H3, 1.102(13); B5−Ha,b,c, 1.12 (avg); N2−Ha,b, 0.88 (avg); N4−Ha,b, 0.87 (avg); N6−Ha,b, 0.87 (avg); B1−N2−B3, 117.78(10); N2−B3−N4, 107.56(10); B3−N4−B5, 118.10(10); N4−B3−N6, 109.55(10); B5−N4−B3, 117.63(9).

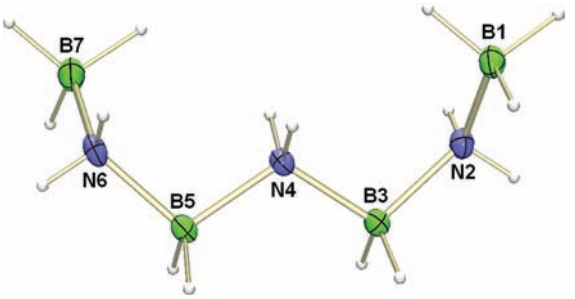

Figure 4. Crystallographically determined structure of the seven-membered linear-chain aminoborane anion in **2b**. Selected bond distances (Å) and angles (deg): B1−N2, 1.5845(16); N2−B3, 1.575(16); B3−N4, 1.5729(15); N4−B5, 1.5795(15); B5−N6, 1.5711(15); N6−B7, 1.5902(16); B1−Ha,b,c, 1.14 (avg); B7−Ha,b,c, 1.14 (avg); B3−Ha,b, 1.13 (avg); B5−Ha,b, 1.12 (avg); N2−Ha,b, 0.86 (avg); N4−Ha,b, 0.87 (avg); N6−Ha,b, 0.83 (avg); B1−N2−B3, 118.81(9); N2−B3−N4, 108.90(9); B3−N4−B5, 116.73(9); N4−B5−N6, 107.67(9); B5−N6−B7, 117.63(9).

^{11}B NMR spectrum of **1** (Figure 5, top) shows an intensity-1 triplet resonance at −8.8 ppm arising from the internal BH_2 group and an intensity-2 quartet resonance at −22.3 ppm arising from the terminal BH_3 groups. The ^{11}B NMR spectrum (Figure 5, bottom) of the seven-membered linear chain **2b** is similar to that of **1**, except that the two resonances are of equal intensity and the BH_2 triplet is shifted upfield to −10.7 ppm. The spectrum of the branched isomer **2a** (Figure 5, middle) displays the expected doublet arising from the central BH group, which is shifted downfield (−4.5 ppm) relative to the triplet resonances of the linear compounds; the quartet of the terminal BH_3 groups is shifted upfield to −24.0 ppm. The experimentally observed ^{11}B NMR shifts of all three anions

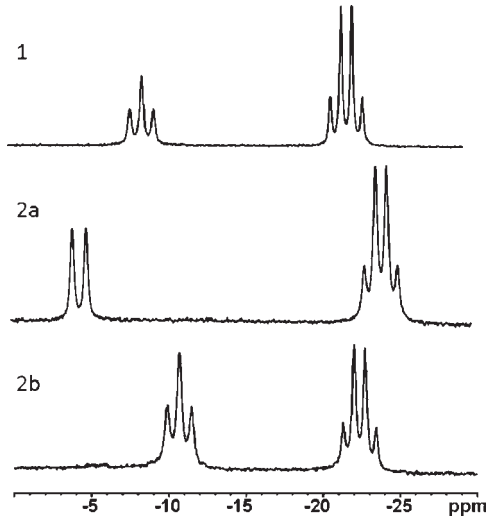

Figure 5. ^{11}B NMR spectra of **1**, **2a**, and **2b**.

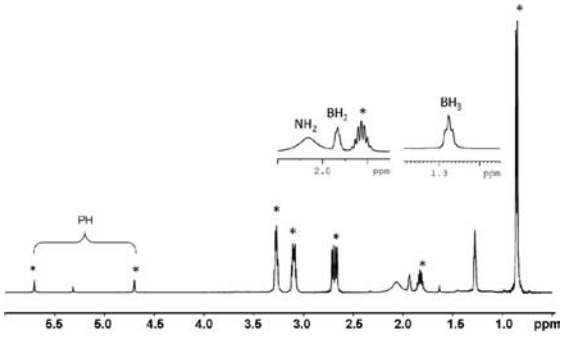

Figure 6. $^{1}H\{^{11}B\}$ NMR spectrum of **1** (in CD_2Cl_2). Asterisks indicate resonances arising from the VBH^+ cation.[8]

are in good agreement with their DFT/GIAO-calculated values (Table S2 in the SI).

As can be seen in Figure 6, the $^{1}H\{^{11}B\}$ NMR spectrum of **1** shows, in addition to the resonances of the VBH^+ cation,[8] a broad resonance of intensity-4 at 2.07 ppm assignable to the NH_2 protons along with intensity-6 and -2 resonances at 1.28 and 1.93 ppm, respectively, arising from the BH_3 and BH_2 protons. The fine quintet coupling ($J = \sim 5$ Hz) of the 1.93 ppm resonance and the triplet coupling ($J = \sim 5$ Hz) of the 1.28 ppm resonance, along with the conversion of these resonances to broad quartets in the boron-coupled ^{1}H NMR spectra, supports their assignments as the BH_2 and BH_3 units that are adjacent to two NH_2 groups and one NH_2 group, respectively. The resonances of the boron and nitrogen hydrogens in the $^{1}H\{^{11}B\}$ NMR spectra of **2a** and **2b** (Figures S7 and S8 in the SI) likewise occur in the expected shift ranges with intensities in accord with their proposed structures.

Crabtree[19] has shown that intermolecular dihydrogen bonding between hydridic B−H (δ^-) and protonic N−H (δ^+) hydrogens is important for "BNH" compounds. In the solid state, the B−H···H−N dihydrogen-bonding distances are typically 1.7−2.2 Å, and in contrast to classical hydrogen-bonding interactions, the B−H···H−N unit is not linear, with the H···H−N angles (117−171°) usually larger than the B−H···H angles (95−120°). The ORTEP plots presented in Figure 7 show the relative orientation of the linear anionic

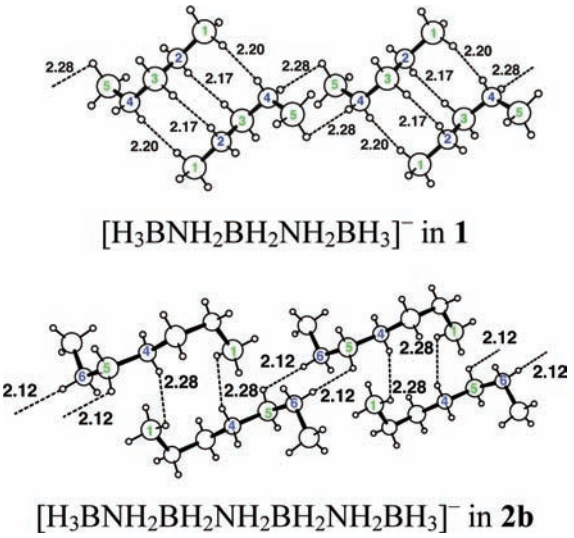

Figure 7. Distances (Å) and angles (deg) for the closest interanionic B−H···H−N interactions in the crystallographically determined structures of **1** and **2b**. **1**: H2b···H3b, 2.17(2); N2−H2b···H3b, 165(1); H2b···H3b−B3, 121(1); H1c···H4b, 2.20(2); B1−H1c···H4b, 114(1); H1c···H4b−N4, 167(2); H4a···H5a, 2.28(2); N4−H4a···H5a, 160(1); H4a···H5a−B5, 101(1). **2b**: H5b···H6b, 2.12(2); B5−H5b···H6b, 116.2(7); H5b···H6b−N6, 175.6(11); H1a···H4b, 2.28(2); B1−H1a···H4b, 107.2(7); H1a···H4b-N4, 160.5(11).

chains in the crystal structures of **1** and **2b**. In both **1** and **2b**, the N−H and B−H hydrogens on one chain are respectively oriented toward B−H and N−H hydrogens on adjacent chains, indicating significant intermolecular B−H···H−N dihydrogen-bonding interactions. The H3b···H2b distance [2.17(2) Å] and N2−H2b···H3b [165(1)°] and B3−H3b···H2b [121(1)°] bond angles for **1** and the H5b···H6b distance [2.12(2) Å] and N6−H6b···H5b [175(6)°] and B5−H5b···H6b [116.2(7)°] bond angles for **2b** are all in the ranges previously found[19] for molecules having strong B−H···H−N dihydrogen-bonding interactions. Although not exhibiting the extensive anion interactions found in **1** and **2b**, the packing diagram for **2a** (Figure S11 in the SI) exhibits at least one strong N−H···H−B interaction between the $HB(NH_2BH_3)_3^-$ anions, with a H2b···H7a distance of 2.19(2) Å and N2−H2b···H7a and B7−H7a···H2b bond angles of 133(1) and 103.1(9)°, respectively.

Girolami[20] has recently reported that while the room-temperature reactions of Na or $NaNH_2$ with AB in THF initially yield the $Na^+[H_3BNH_2]^-$ salt, heating the reactions causes further reaction with another AB equivalent to form $Na^+[H_3BNH_2BH_3]^-$, which then precipitates from the solution. Similar steps in the VB/AB reactions (eqs 3 and 4) would produce VBH^+-$[H_3BNH_2BH_3]^-$:

$$H_3BNH_3 + VB \rightarrow VBH^+[H_3BNH_2]^- \quad (3)$$

$$VBH^+[H_3BNH_2]^- + H_3BNH_3 \rightarrow VBH^+[H_3BNH_2BH_3]^- + NH_3 \quad (4)$$

The organic VBH^+ cation keeps the $VBH^+[H_3BNH_2BH_3]^-$ salt in solution, thereby facilitating its further reaction. The fact that

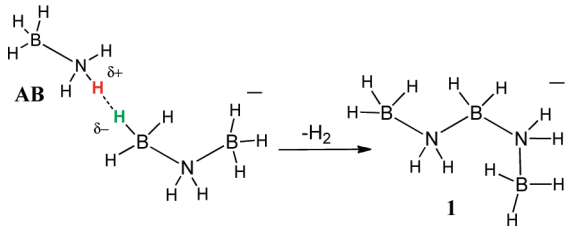

Figure 8. Possible dehydrocoupling pathway leading to the formation of **1** from AB and $[H_3BNH_2BH_3]^-$.

$[VBH^+][H_3BNH_2BH_3]^-$ was not observed by NMR analysis suggests that it readily dehydrocouples with an additional AB to yield the stable observed product $VBH^+[H_3BNH_2BH_2NH_2BH_3]^-$ (eq 5).

$$VBH^+[BH_3NH_2BH_3]^- + H_3NBH_3 \rightarrow VBH^+[H_3BNH_2BH_2NH_2BH_3]^- + H_2 \quad (5)$$

A dehydrocoupling step leading to the formation of **1**, such as the one depicted in Figure 8, which involves interionic elimination of a protonic N−H on AB with the hydridic B−H of the $H_3BNH_2BH_3^-$ anion, is supported by our earlier studies[5a] of the reactions of AB with $Li^+[Et_3BNH_2BH_3]^-$, formed by the dehydrocoupling of AB with $Li^+[Et_3BH]^-$. Those studies provided NMR and mass spectral evidence for the formation of the chain-growth product $Li^+[Et_3BNH_2BH_2NH_2BH_3]^-$ at room temperature (eq 6) and longer oligomeric anionic aminoboranes at higher temperatures with excess AB.

$$Li^+[Et_3BNH_2BH_3]^- + H_3NBH_3 \rightarrow Li^+[Et_3BNH_2BH_2NH_2BH_3]^- + H_2 \quad (6)$$

A subsequent dehydrocoupling step in the VB/AB reactions involving chain growth from **1** to **2a** and **2b** was confirmed by the results of a reaction of **1** with an additional AB equivalent (eq 7):

$$VBH^+[H_3BNH_2BH_2NH_2BH_3]^- + H_3NBH_3 \rightarrow VBH^+[HB(NH_2BH_3)_3]^- + VBH^+[H_3BNH_2BH_2NH_2BH_2NH_2BH_3]^- + H_2 \quad (7)$$

After 2 days at 50 °C, ^{11}B NMR analysis (Figure S10 in the SI) indicated the formation of a mixture containing the aminoborane anions in ratios similar to those observed in the reaction of VB with 4 equiv of AB. These results support a second chain-growth step such as the one depicted in Figure 9, where the interionic elimination of a protonic N−H on AB with one of the internal BH_2 hydridic hydrogens of **1** would yield **2a**, while the reaction of an AB with one of the terminal BH_3 hydrides of **1** would give **2b**.

Reactions at 50 °C also always produced a small amount (<20 mg) of a white solid that, unlike **2a** and **2b**, was insoluble in CH_2Cl_2. The ^{11}B NMR spectrum of this material dissolved in DMF (Figure S9 in the SI) showed, in addition to BH_3 and BH resonances, larger peaks in the −10 to −14 ppm region where internal BH_2 resonances are found, suggesting the formation of higher chain-growth oligomers. Because of their higher AB/base ratios and temperatures, base-promoted AB H_2 release reactions, such as the examples in Figure 1, employing only 5 mol % (i.e., a 20:1 AB/base ratio) or less base carried out at 85 °C likely produce even larger oligomers. Supporting this conclusion is our previous observation[5] that the ^{11}B NMR spectra of the soluble product mixtures formed during the initial stages of AB H_2 release reactions (up to the loss of 1−1.2 equiv of H_2) always showed progressive growth of resonances in the BH_2 regions as the reaction proceeded. As these reactions progressed to the loss of ∼2 equiv of H_2, the products became increasingly insoluble. Analysis by solid-state ^{11}B NMR spectroscopy showed that the final insoluble products contained only sp^2-hybridized boron.[5] Thus, in the final stages of the AB H_2 release reactions, dehydrogenation of the initially formed sp^3-hybridized anionic polyaminoboranes must occur by a different mechanistic pathway that involves cyclization and formation of B═N unsaturation and ultimately yields spent-fuel materials with polyborazylene-type sp^2-hybridized structures.

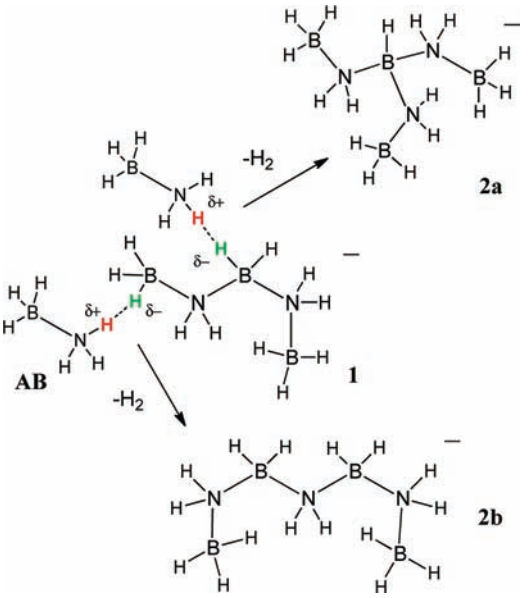

Figure 9. Two possible pathways for chain growth leading to the formation of **2a** and **2b** via the dehydrocoupling of **1** and AB.

CONCLUSION

The use of the strong organic base VB as an initiator has allowed the syntheses and structural characterizations of new five- and seven-membered borane-capped anionic aminoborane oligomers that are likely early intermediates in base-promoted ammonia borane H_2 release reactions. Sequential H_2 elimination reactions leading to chain growth are likely facilitated by N−H···H−B dihydrogen-bonding interactions between the AB N−H protonic hydrogens and the hydridic B−H hydrogens of the growing anionic aminoborane chains. These results provide direct support for an anionic chain-growth mechanism as an initial step in base-promoted AB H_2 release reactions and further illustrate that AB H_2 release reactions are complex, with the many possible mechanistic steps for AB H_2 release determined by both the method of AB activation and the reactivity differences of the resulting intermediate species.

ASSOCIATED CONTENT

Supporting Information. Tables of IR spectra and DFT/GIAO-calculated ^{11}B NMR shifts for **1**, **2a**, and **2b**; DFT-optimized geometries and their Cartesian coordinates; relative energies of DFT-optimized geometries; $^1H\{^{11}B\}$ NMR spectra for **2a** and **2b**; ^{11}B NMR spectra of the reaction products of

reactions at 50 °C; a diagram showing the closest B−H···H−N interactions in the crystal structure of **2a**; and complete ref 10. This material is available free of charge via the Internet at http://pubs.acs.org.

AUTHOR INFORMATION

Corresponding Author
lsneddon@sas.upenn.edu

ACKNOWLEDGMENT

We gratefully acknowledge the U.S. Department of Energy for support of this research and the National Science Foundation for an instrumentation grant (CHE−0840438) used for the purchase of the X-ray diffractometer employed in these studies.

REFERENCES

(1) (a) Sutton, A. D.; Burrell, A. K.; Dixon, D. A.; Garner, E. B., III; Gordon, J. C.; Nakagawa, T.; Ott, K. C.; Robinson, J. P.; Vasiliu, M. *Science* **2011**, 1426–1429. (b) Davis, B. L.; Dixon, D. A.; Garner, E. B.; Gordon, J. C.; Matus, M. H.; Scott, B. L.; Stephens, F. H. *Angew. Chem., Int. Ed.* **2009**, *48*, 6812–6816. (c) Sutton, A. D.; Ellis, B. E.; Gordon, J. C.; Power, P. P. *Chem. Commun.* **2010**, *46*, 148–152.

(2) For some recent reviews of the properties of AB, see: (a) Stephens, F. H.; Pons, V.; Baker, R. T. *Dalton Trans.* **2007**, 2613–2626. (b) Marder, T. B. *Angew. Chem., Int. Ed.* **2007**, *46*, 8116–8118. (c) Peng, B.; Chen, J. *Energy Environ. Sci.* **2008**, *1*, 479–483. (d) Hamilton, C. W.; Baker, R. T.; Staubitz, A.; Manners, I. *Chem. Soc. Rev.* **2009**, *38*, 279–296. (e) Staubitz, A.; Robertson, A. P. M.; Manners, I. *Chem. Rev.* **2010**, *110*, 4079–4124. (f) Bowden, M.; Autrey, T. *Curr. Opin. Solid State Mater. Sci.* **2011**, *15*, 73–79.

(3) (a) Gutowska, A.; Li, L.; Shin, Y.; Wang, C. M.; Li, X. S.; Linehan, J. C.; Smith, R. S.; Kay, B. D.; Schmid, B.; Shaw, W.; Gutowski, M.; Autrey, T. *Angew. Chem., Int. Ed.* **2005**, *44*, 3578–3582. (b) Sepehri, S.; Feaver, A.; Shaw, W. J.; Howard, C. J.; Zhang, Q.; Autrey, T.; Cao, G. *J. Phys. Chem. B* **2007**, *111*, 14285–14289. (c) Paolone, A.; Palumbo, O.; Rispoli, P.; Cantelli, R.; Autrey, T.; Karkamkar, A. *J. Phys. Chem. C* **2009**, *113*, 10319–10321.

(4) Stephens, F. H.; Baker, R. T.; Matus, M. H.; Grant, D. J.; Dixon, D. A. *Angew. Chem., Int. Ed.* **2007**, *46*, 746–749.

(5) (a) Himmelberger, D. W.; Yoon, C. W.; Bluhm, M. E.; Carroll, P. J.; Sneddon, L. G. *J. Am. Chem. Soc.* **2009**, *131*, 14101–14110. (b) Himmelberger, D. W.; Bluhm, M. E.; Sneddon, L. G. *Prepr. Symp.—Am. Chem. Soc., Div. Fuel Chem.* **2008**, *53*, 666–667.

(6) (a) Bluhm, M. E.; Bradley, M. G.; Butterick, R., III; Kusari, U.; Sneddon, L. G. *J. Am. Chem. Soc.* **2006**, *128*, 7748–7749. (b) Himmelberger, D. W.; Alden, L. R.; Bluhm, M. E.; Carroll, P. J.; Sneddon, L. G. *Inorg. Chem.* **2009**, *48*, 9883–9889.

(7) For some recent reviews of metal-catalyzed AB reactions, see ref 2 and: Alcaraz, G.; Sabo-Etienne, S. *Angew. Chem., Int. Ed.* **2010**, *49*, 7170–7179.

(8) Kisanga, P. B.; Verkade, J. G. *Tetrahedron* **2001**, *57*, 467–475.

(9) Shriver, D. F.; Drezdzon, M. A. *The Manipulation of Air-Sensitive Compounds*, 2nd ed.; Wiley: New York, 1996.

(10) Frisch, M. J; et al. *Gaussian 03*, revision B.05; Gaussian, Inc.: Pittsburgh PA, 2003.

(11) *SAINT*, version 7.68A; Bruker AXS Inc.: Madison, WI.

(12) *SHELXTL*, version 6.14; Bruker AXS Inc.: Madison, WI.

(13) *SADABS*, version 2008/1; Bruker AXS Inc.: Madison, WI.

(14) SIR97: Altomare, A.; Burla, M. C.; Camalli, M.; Cascarano, M.; Giacovazzo, C.; Guagliardi, A.; Moliterni, A.; Polidori, G. J.; Spagna, R. *J. Appl. Crystallogr.* **1999**, *32*, 115–119.

(15) Sheldrick, G. M. *Acta Crystallogr.* **2008**, *A64*, 112–122.

(16) For a review of the properties of Verkade-type bases, see: Verkade, J. G.; Kisanga, P. B. *Tetrahedron* **2003**, *59*, 7819–7858.

(17) Heating at 50 °C is not sufficient to induce significant thermal dehydropolymerization of AB. See: Shaw, W. J.; Linehan, J. C.; Szymczak, N. K.; Heldebrant, D. J.; Yonker, C.; Camaioni, D. M.; Baker, R. T.; Autrey, T. *Angew. Chem., Int. Ed.* **2008**, *47*, 7493–7496.

(18) Chen, X.; Zhao, J.-C.; Shore, S. G. *Inorg. Chem.* **2010**, *132*, 10658–10659.

(19) (a) Richardson, T. B.; Gala, S. D.; Crabtree, R. H. *J. Am. Chem. Soc.* **1995**, *117*, 12875–12876. (b) Crabtree, R. H.; Siegbahn, P. E. M.; Eisenstein, O.; Rheingold, A. L.; Koetzle, T. F. *Acc. Chem. Res.* **1996**, *29*, 348–354. (c) Klooster, W. T.; Koetzle, T. F.; Siegbahn, P. E. M.; Richardson, T. B.; Crabtree, R. H. *J. Am. Chem. Soc.* **1999**, *121*, 6337–6343.

(20) Daly, S. R.; Bellott, B. J.; Kim, D. Y.; Girolami, G. S. *J. Am. Chem. Soc.* **2010**, *132*, 7254–7255.